Proceedings of the 21st ICSMGE, Vienna, Austria, 14 – 19 June 2026. Pistrol, Adam & Schweiger (eds.)
Published by: ÖGG, Austrian Society for Geomechanics, Salzburg, Austria, ISBN 978-3-9503898-4-5
https://doi.org/10.53243/ICSMGE2026-145

Instability of partially saturated silty sand under suction-controlled constant shear drained condition

Shafna Kaliparambil Jamal, Jayan S. Vinod, Kumari W.G.P, Partha Narayan Mishra
Faculty of Engineering and Information Sciences, University of Wollongong, NSW 2522, Australia
vinod@uow.edu.au

ABSTRACT: The stability of geotechnical structures such as slopes, embankments, and stockpiles is often governed by the behavior of partially saturated soil, as these structures typically exist above the ground water table. The matric suction (Ψ_m) plays a key role in predicting the strength and deformation behaviour of partially saturated soil. Moreover, the change in Ψ_m has a significant influence on the instability of partially saturated soil. However, the precise prediction on the onset of instability in partially saturated condition remains a challenge due to the associated Ψ_m. This study investigates the instability behavior of partially saturated silty sand with different Ψ_m under the Constant Shear Drained (CSD) condition, which replicates the field condition during rainfall infiltration scenarios where, deviator stress remain constant while mean net/effective stress reduces. The findings indicate that the onset of instability decreases with a decrease in Ψ_m, reflecting the reduction in the stability of soil as rainfall infiltrates the soil. The onset of instability is higher for the silty sand compacted to optimum moisture content (OMC) than that of wet of OMC with the imposition of the same Ψ_m. Additionally, partially saturated silty sand exhibited dilative volume change behavior at different Ψ_m values, density and moisture conditions, in contrast to the contractive behaviour under fully saturated conditions. Existing methods for identifying the onset of instability, originally developed for the fully saturated condition, were extended to determine the onset of instability in partially saturated silty sand under the CSD condition. A unique onset of instability was identified for partially saturated silty sand under the CSD condition irrespective of different approaches considered in this study.

KEYWORDS: Partially saturated silty sand, Matric suction, Constant shear drained condition.

1 INTRODUCTION

Most geotechnical structures, such as retaining walls, embankments, roads, and slopes, are constructed above the groundwater table, where soils exist in a partially saturated condition. The mechanical behaviour of partially saturated soils is more complex and less predictable than fully saturated soils due to the presence of both water and air phases and the resulting matric suction (Ψ_m), defined as the difference of pore air and pore water pressure (Wang et al. 2002). This Ψ_m influences both strength and deformation behaviour and plays a vital role in governing partially saturated soil response. The concept of effective stress in partially saturated soils is more complex than in saturated soil and has been interpreted through various theoretical frameworks. Bishop (1959) proposed an extended effective stress equation incorporating net stress and matric suction as a single stress state variable.

$$\sigma' = (\sigma - u_a) + \chi\,(u_a - u_w) \quad (1)$$

where σ, σ', χ, $(u_a - u_w)$ are total stress, effective stress, effective stress parameter, and Ψ_m respectively. Later, Fredlund and Morgenstern (1977) treated net stress and matric suction as two independent stress state variables. Each of these frameworks has offered distinct perspectives on the behaviour of partially saturated soil, but matric suction is a key parameter influencing the soil behaviour.

Laboratory testing plays a key role in understanding the mechanical behaviour and validation of the theoretical frameworks of partially saturated soil. Among these, triaxial testing is one of the most widely used methods for evaluating the mechanical behaviour of partially saturated soils. Triaxial tests on partially saturated soils are commonly performed under conventional stress paths such as Consolidated Drained (CD) or Consolidated Undrained (CU) conditions, for varying net stresses and Ψ_m, to evaluate the behavior (e.g. Thu et al. 2007). These tests are critical for evaluating key geotechnical shear strength parameters and stiffness characteristics. However, they may not fully capture the progressive failure mechanisms and instability behaviour observed in the field, particularly under rainfall infiltration conditions.

In field, soil elements on slopes affected by rainfall infiltration or a rising phreatic surface may experience a Constant Shear Drained (CSD) stress path rather than a conventional drained or undrained stress path (e.g. Dong et al. 2015). The CSD stress path is characterized by a gradual reduction in net or effective stress while maintaining a constant deviator stress, potentially leading to failure even without additional external loading. The modelling of instability in granular soils subjected to CSD stress paths remains fundamentally different from that in conventional testing under drained or undrained conditions, which are primarily governed by loading and drainage conditions.

Ψ_m varies continuously as rainfall infiltrates the dry soil, highlighting the need to accurately capture the onset of instability in partially saturated soils under CSD conditions with different Ψ_m values. While numerous studies have focused on fully saturated soils under the CSD condition (e.g. Monkul et al. 2011), their direct application to partially saturated soils remain limited due to the additional complexities introduced by Ψ_m and partial saturation. Various techniques have been widely employed to capture the onset of instability in fully saturated soils under CSD testing. However, despite their potential significance, their application to partially saturated soils are still relatively limited.

Therefore, this study aims to address this problem by examining the influence of Ψ_m on the onset of instability of partially saturated silty sand under the CSD stress path testing. It offers insights that are critical for advancing predictive numerical models by incorporating Ψ_m -dependent instability criteria into constitutive frameworks. These improvements enable better simulation of rainfall-induced failures in partially saturated slopes and for risk assessment including the development of any early warning systems to notify the critical risk levels on slopes. These are essential for risk mitigation, particularly in infrastructure built on or near partially saturated slopes, stockpiles, and embankments exposed to changing hydrological conditions.

2 MATERIALS AND METHODS

The suction-controlled triaxial tests were carried out using the HKUST (Hong Kong University of Science and Technology) double-walled triaxial system under CSD conditions. The base pedestal of the conventional triaxial equipment was modified with the inclusion of a High Air Entry (HAE) ceramic disc having a capacity of 1500 kPa. The saturation of the HAE disc was achieved by introducing pressurised water to pass through it for at least 12 hours before beginning the suction equalisation, suction-controlled consolidation, and shearing. It is an advanced apparatus designed for testing the behaviour of partially saturated soil, which can control the pore air pressure and pore water pressure independently (e.g Houston et al. 2008). Servo-controlled triaxial load frame with a maximum axial displacement rate of 0.15 mm/min was used in this study.

The silty sand used for this study was collected from the banks of Mullet Creek, NSW, Australia. A series of suction-controlled triaxial tests were conducted under CSD condition to investigate the effect of suction on the onset of instability. Figure 1 shows the particle size distribution (PSD) curve of the soil obtained from the laser analysis. The samples (50 mm x 100 mm) for triaxial tests were prepared at both OMC (maximum dry density, γ_d max = 16.80 kN/m^3 and moisture content, w at γ_d max = 14 %) and wet side of the peak of compaction curve (dry density, γ_d = 16.10 kN/m^3 and corresponding moisture content, w = 16 %). The wet side of optimum replicates the post- rainfall infiltration condition in the field, and it will prevent the formation of aggregate fabric, which makes the particles roll over one another rather than slide (Banerjee et al. 2020).

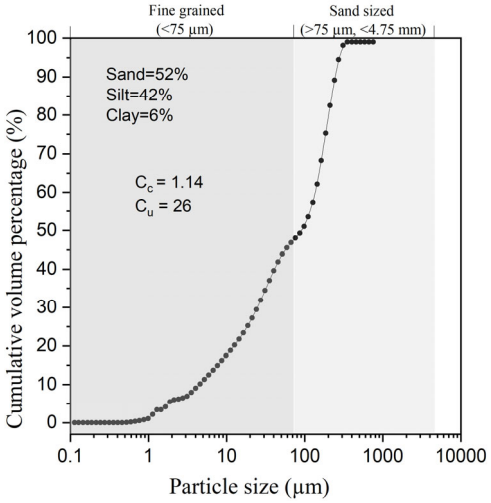

Figure 1. Particle size distribution of silty sand (Modified after Jamal et al.2025)

Ψ_m values (0, 25, 50, and 100 kPa) were chosen from the transition zone of the soil water retention curve SWRC (Figure 2) obtained from the contact filter paper method (ASTM D5298 -16.2016) and Van Genutchen (1980) model fitting (Equation (1)).

$$\theta = \theta_r + \frac{\theta_s - \theta_r}{(1 + \alpha \Psi m^n)^m} \quad (2)$$

where θ, θ_r, θ_s are the normalized water content, water content at residual and saturated states, respectively. α, n, m are the fitting parameters with $m = 1 - \frac{1}{n}$.

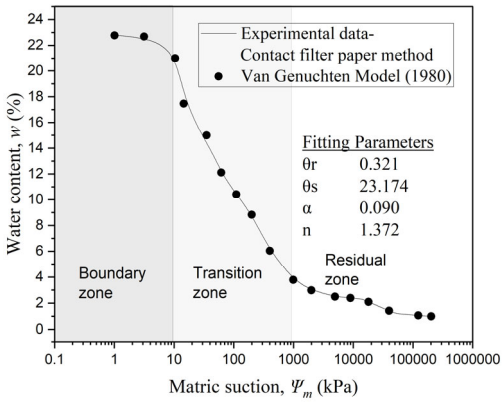

Figure 2. SWRC of silty sand

The Ψ_m was imposed in the sample using the axis translation technique rather than being measured directly. The control of Ψ_m was achieved by monitoring the pressure difference between the advanced pore air and pore water pressure controllers. The suction equalisation was considered finished after there was negligible flow of water into or out of the soil, or less than 0.1 cm^3 per day. Air flushing is one of the critical steps in the testing of partially saturated soil, which maintains a proper and clear pore air network by ensuring proper entrapped air drainage from the bottom of the HAE disc. Air-flushing under the HAE ceramic disc was done at all times during testing using the drainage lines through the bottom of the HAE disc and it was maintained by a controlled flow of de-aired water (Cai et al.2022)

Initially, the sample was consolidated to a mean effective stress ($p'_{eff} = \frac{\sigma_1+\sigma_2+\sigma_3}{3} - u_w$) of 100 kPa in the saturated state or to a mean net stress ($p'_{net} = \frac{\sigma_1+\sigma_2+\sigma_3}{3} - u_a$) of 100 kPa in the partially saturated state. σ_1, σ_2, σ_3 represent the principal stresses and u_a, u_w denote pore air and pore water pressure, respectively. The sample was sheared under consolidated drained (CD) test to a deviator stress (q) of 100 kPa (e.g. Ahmed et al. 2022).

The CSD tests were conducted by reducing the $p'_{eff/net}$ at a rate of 10 kPa/h (e.g. Rabbi et al. 2019) for various Ψ_m until the silty sand exhibited the onset of instability. The $p'_{eff/net}$ was controlled in the sample through an independent regulation of total and pore pressures using advanced controllers. The advanced Differential Pressure Transducer (DPT), along with the servocontrol mechanism incorporated within the equipment, helps to prevent even the slightest fluctuations in the stress condition. The volume transducer designed for partially saturated soil was used for measuring the volume change due to both pore air and pore water pressure.

3 RESULTS AND DISCUSSION

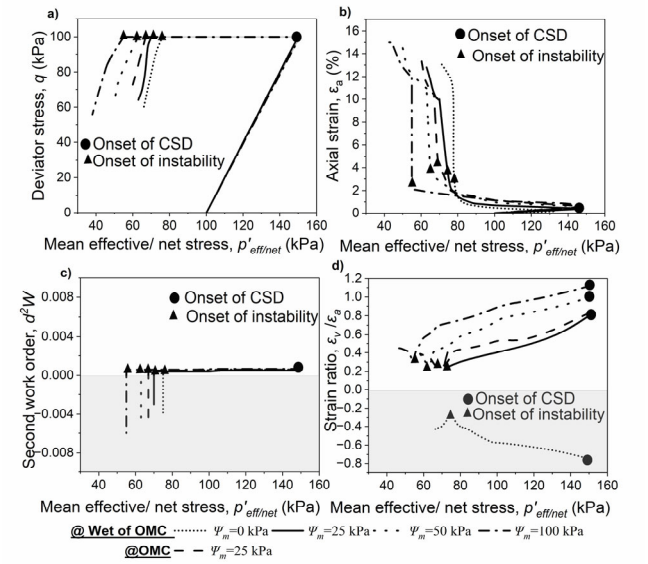

Figure 3. Variation of a) q, b) ε_a, c) d^2w, d) $\varepsilon_v/\varepsilon_a$ with respect to $p'_{eff/net}$ for various Ψ_m

Figure 3a shows the typical behaviour of silty sand in $p'_{eff/net}$ -q space for various Ψ_m under the CSD condition. There is a sharp drop in q along the CSD stress path at a particular $p'_{eff/net}$ identified as the onset of instability, denoted by p'_f. This sharp drop in q, characterized by dq<0 condition, is well established to capture the onset of instability for fully saturated soil under CSD testing (Dong et al.2015) and has been extended here to the partially saturated condition. It is observed from Figure 3a that Ψ_m has a significant influence on p'_f. As Ψ_m increases, p'_f decreases, indicating that $p'_{eff/net}$ reduces further along the CSD stress path before the onset of instability initiates. Moreover, the silty sand compacted on the wet side of OMC exhibits higher p'_f compared to that compacted on OMC. This may be attributed to the strength loss due to increased moisture content.

Figure 3b presents the relationship between the axial strain (ε_a) with respect to $p'_{eff/net}$ for different Ψ_m. At a particular $p'_{eff/net}$ a rapid increase in ε_a is observed, which can lead to collapse, identified as the onset of instability, p'_f. Various researchers used this method to identify the onset of instability for fully saturated soil under CSD testing (Dong et al. 2015). Consistent with Figure 3a, p'_f decreases as Ψ_m increases. Also, the p'_f of silty sand compacted on the wet side of OMC is higher compared to that on OMC, likely due to the moisture-induced softening.

Numerous techniques have been proposed in recent years to identify the onset of soil instability in the CSD stress path. Along with dq<0 and rapid increase in axial strain, the second-order work (d^2w), and strain ratio ($\varepsilon_v/\varepsilon_a$) approach are the widely used methods to capture the onset of instability of saturated soil (Monkul et al.2011).

$$d^2w = dq \times d\varepsilon_a + dp' \times d\varepsilon_v \quad (1)$$

where dq, dp' represent the change in q and $p'_{eff/net}$, respectively. $d\varepsilon_v$, $d\varepsilon_a$ represent the change in ε_v and ε_a, respectively.

Figure 3c shows d^2w approach to find the onset of instability of partially saturated silty sand according to Equation (1). At a particular $p'_{eff/net}$, the d^2w is less than zero, and it is identified as the onset of instability(p'_f). As Ψ_m increases, the p'_f decreases, and it was observed to be higher for the sample compacted at wet of OMC than the OMC.

Figure 3d shows the prediction of the onset of instability in $\varepsilon_v/\varepsilon_a$ - $p'_{eff/net}$ space (Ahmed et al. 2022). It is seen from Figure 3d that the $\varepsilon_v/\varepsilon_a$ for saturated silty sand increases and then shows a sharp drop near the onset of instability (Ahmed et al. 2022). However, for partially saturated silty sand, the $\varepsilon_v/\varepsilon_a$ initially decreases and then increases at the onset of instability. Although the behaviour differs greatly from the saturated state, the $\varepsilon_v/\varepsilon_a$ method is still relevant to silty sand with different Ψ_m values.

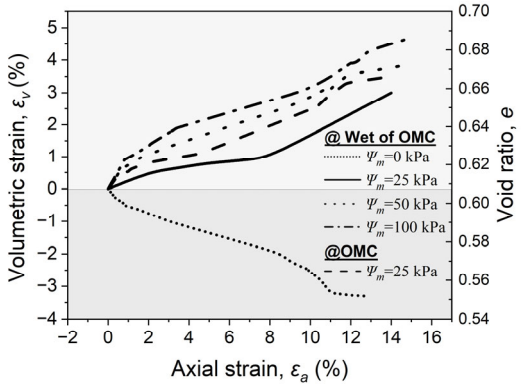

Figure 4. Variation of ε_v/ e with respect to ε_a for various Ψ_m

Figure 4 presents the variation of volumetric strain (ε_v)/ void ratio (e) with ε_a under CSD testing for different Ψ_m. Interestingly, silty sand exhibits a compressive volumetric behaviour in the saturated state, while a dilative response is observed in the partially saturated state. This trend holds for the samples compacted with different densities at OMC and wet of OMC. The dilative behaviour is increasing with an increase in Ψ_m. While the dilative behaviour of partially saturated silty sand under the CSD condition is unique, the compressive volumetric behaviour of fully saturated silty sand under the CSD condition is reported in Rabbi et al. (2019). This contrasting volumetric response may explain the reason for the observed reverse trend in the strain ratio method for saturated and partially saturated states in Figure 3d. The interparticle force (Equation. (1)) arises due to Ψ_m may have contributed to the dilation of silty sand by densifying it in the partially saturated state.

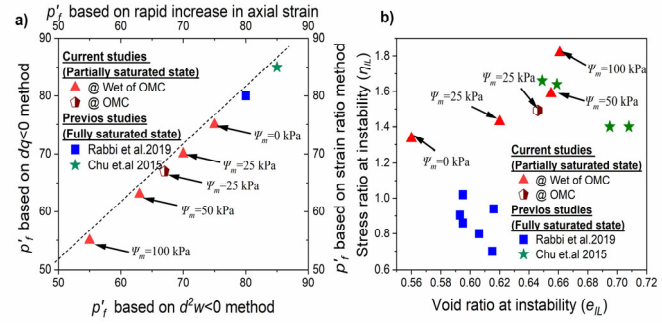

Figure 5. a) p'_f based on different methods, b) Variation of e_{IL} and η_{IL} for different Ψ_m

Figure 5a shows the p'_f captured from different methods. It is evident from Figure 5a that different methods have captured a unique onset of instability irrespective of Ψ_m values. The p'_f

higher for the silty compacted wet of OMC than the OMC. The p'_f decreases, as Ψ_m increases, which is related to the additional contribution of Ψ_m towards the effective stress as per Eq. (1). This behaviour may also be attributed to suction-induced hardening, which effectively shifts the Critical State Line (CSL) upward in e-ln $p'_{eff/net}$ space (e.g. Wheeler & Sivakumar, 1995).

Figure 5b shows the variation of void ratio (e_{IL}) and stress ratio ($\eta_{IL}=q/p'_f$) at the onset of instability. According to Figure 5b, e_{IL} and η_{IL} associated with the onset of instability are higher for the silty sand compacted at OMC than that compacted at wet of OMC. As Ψ_m increases e_{IL} and η_{IL} also increase. The increase in e_{IL} at the onset of instability is related to the dilative behaviour of silty sand in the partially saturated state. The η_{IL}, beyond which the silty sand is unstable, also increases with Ψ_m, due to the corresponding increase in additional contribution towards the effective stress due to Ψ_m. The results of p'_f, e_{IL}, η_{IL} at the onset of instability of the current study are in line with the results of Chu et al. (2015) and Rabbi et al. (2019), which were conducted under CSD testing in a fully saturated state.

4 CONCLUSIONS

This study on the instability behavior of silty sand in partially saturated condition shows that Ψ_m has a significant influence on the onset of instability under the CSD condition. It was observed that as Ψ_m increases, p'_f, corresponding to the onset of instability decreases, indicating that the silty sand can better sustain loading along the CSD stress path before the failure. This behaviour may be due to the additional contribution of Ψ_m towards the net stress as shown in Equation 1. The lower p'_f for the silty sand sample compacted to OMC compared to that prepared at wet of OMC with the imposition of the same Ψ_m is attributed due to the strength loss associated with the increased moisture content.

The experimental results show that the volumetric behaviour is dilative and compressive in partially saturated conditions and in fully saturated condition, respectively under the CSD testing for silty sand compacted with different densities (e.g. wet of OMC and OMC). The study further showcases that techniques such as d^2w, dq <0, rapid increase in ε_a and $\varepsilon_v/\varepsilon_a$ approach can be extended to capture the onset of instability in partially saturated silty sand, which has previously been explored extensively only for fully saturated conditions. A unique onset of instability of silty sand was observed using distinct approaches and it increases with the increase in Ψ_m. As Ψ_m increases, e_{IL} and η_{IL} also increase, which is related to the dilative behaviour of silty sand in the partially saturated state and the developed additional effective stress due to Ψ_m respectively.

5 ACKNOWLEDGEMENTS

The first author acknowledges the PhD scholarship support from the University of Wollongong (UoW), Australia. The authors also acknowledge Mr. Richard Berndt, senior technical officer (UoW), for his assistance with the experiments.

6 REFERENCES

Ahmed, S., Vinod, J.S., Sheikh, M.N., Fourie, A., and Reid, D. 2022. The εv/εa–p′ method for the determination of instability of granular soils under constant shear drained stress path. Canadian Geotechnical Journal, 59(8), 1527–1530.

ASTM, International. 2016. Standard test method for measurement of soil potential (suction) using filter paper. ASTM D5298-16

Banerjee, A., Puppala, A.J., and Hoyos, L.R. 2020. Suction-controlled multistage triaxial testing on clayey silty soil. Engineering geology, 265, 105409.

Bishop, A. W. 1959. The Principles of Effective Stress. Teknisk Ukeblad 106, no. 39 (January): 859–863.

Cai, G., Han, B., Asreazad, S., Liu, C., Zhou, A., Li, J., and Zhao, C. 2022. Experimental study on critical state behavior of unsaturated silty sand under constant matric suctions. Géotechnique, vol. 74, no. 5, pp. 409–430.

Chu, J., Wanatowski, D., Leong, W.K., Loke, W.L., and He, J. 2015. Instability of dilative sand. Geotechnical Research, 2(1), 35–48.

Dong, Q.C., Xu, C., Cai, Y., Juang, H., Wang, J., Yang, Z., and Gu, C. 2015. Drained instability in loose granular material. International Journal of Geomechanics, 16 (2), 04015043.

Fredlund, D. G., and Morgenstern, N.R. 1977. Stress state variables for unsaturated soils. Canadian Geotechnical Journal, 16,121–139.

Genutchen, V. 1980. A close form equation for predicting the water permeability of unsaturated soils. Journal of Soil science, 44,892-898.

Houston, S.L., Perez-Garcia, N., Houston, W.N., 2008. Shear strength and shear-induced volume change behaviour of unsaturated soils from a Triaxial test program. J. Geotech. Geoenviron. Eng. 134 (11), 1619–1632.

Monkul, M., Yamamuro, J.A., and Lade, P.V. 2011. Failure, instability, and the second work increment in loose silty sand,Canadian Geotechnical Journal, 48(6),943-955.

Rabbi, A. T. M. Z., Rahman, M.M., and Cameron, D. 2019. Critical state study of natural silty sand instability under undrained and constant shear drained path. International Journal of Geomechanics. Vol 19(8), 04019083

Jamal, S.K., Vinod, J.S., W.G.P Kumari., Mishra P.N. 2025. Effect of suction on the instability of silty sand under constant shear drained testing. Canadian Geotechnical Journal, 62, 1-5.

Thu, T., Rahardjo, H., and Leong, E.C. 2007. Critical State Behavior of a Compacted Silt Specimen. Soils and Foundations, 47(4), 749–755.

Wang, Q., Pufahl, D.E., and Fredlund, D.G. 2002. A study of critical state on an unsaturated silty soil. Canadian Geotechnical Journal, 39(1), 213–218.

Wheeler, S.J., & Sivakumar, V. 1995. An elasto-plastic critical state framework for unsaturated soil, Geotechnique, 45(1), 35-53.